

Experimental demonstration of a fast calibration method for integrated photonic circuits with cascaded phase shifters

Junqin Cao(曹君勤), Zhixin Chen(陈志歆), Yaxin Wang(王亚新), Tianfeng Feng(冯田峰), Zhihao Li(李志浩), Zeyu Xing(邢泽宇), Huashan Li(李华山), and Xiaoqi Zhou(周晓祺)

Citation: Chin. Phys. B, 2022, 31 (**11**): 114204. DOI: 10.1088/1674-1056/ac8737

What follows is a list of articles you may be interested in

Precise determination of characteristic laser frequencies by an Er-doped fiber optical frequency comb

Shiying Cao(曹士英), Yi Han(韩羿), Yongjin Ding(丁永今), Baike Lin(林百科), and Zhanjun Fang(方占军)

Chin. Phys. B, 2022, 31 (**7**): 074207. DOI: 10.1088/1674-1056/ac5608

A pressure-calibration method of wavelength modulation spectroscopy in sealed microbial growth environment

Kun-Yang Wang(王坤阳), Jie Shao(邵杰), Li-Gang Shao(邵李刚), Jia-Jin Chen(陈家金), Gui-Shi Wang(王贵师), Kun Liu(刘琨), and Xiao-Ming Gao(高晓明)

Chin. Phys. B, 2021, 30 (**5**): 054203. DOI: 10.1088/1674-1056/abda32

A fast and precise three-dimensional measurement system based on multiple parallel line lasers

Yao Wang(王尧) and Bin Lin(林斌)

Chin. Phys. B, 2021, 30 (**2**): 024201. DOI: 10.1088/1674-1056/abc14d

Design and optimization of microstructure optical fiber sensor based on bimetal plasmon mode interaction

Meng Wu(吴萌), Xin-Yu Liu(刘欣宇), Gui-Yao Zhou(周桂耀), Chang-Ming Xia(夏长明), Bo-Yao Li(李波瑶), Zhi-Yun Hou(侯峙云)

Chin. Phys. B, 2019, 28 (**12**): 124202. DOI: 10.1088/1674-1056/ab4d48

Characterization of focusing performance of spiral zone plates with fractal structure

Hua-Ping Zang(臧华平), Cheng-Long Zheng(郑程龙), Zi-Wen Ji(吉子雯), Quan-Ping Fan(范全平), Lai Wei(魏来), Yong-Jie Li(李永杰), Kai-Jun Mu(牧凯军), Shu Chen(陈述), Chuan-Ke Wang(王传珂), Xiao-Li Zhu(朱效力), Chang-Qing Xie(谢常青), Lei-Feng Cao(曹磊峰), Er-Jun Liang(梁二军)

Chin. Phys. B, 2019, 28 (**6**): 064201. DOI: 10.1088/1674-1056/28/6/064201

Experimental demonstration of a fast calibration method for integrated photonic circuits with cascaded phase shifters

Junqin Cao(曹君勤)[†], Zhixin Chen(陈志歆)[†], Yaxin Wang(王亚新), Tianfeng Feng(冯田峰), Zhihao Li(李志浩), Zeyu Xing(邢泽宇), Huashan Li(李华山), and Xiaoqi Zhou(周晓祺)[‡]

School of Physics and State Key Laboratory of Optoelectronic Materials and Technologies, Sun Yat-sen University, Guangzhou 510000, *China*

(Received 2 June 2022; revised manuscript received 20 July 2022; accepted manuscript online 5 August 2022)

With the development of research on integrated photonic quantum information processing, the integration level of the integrated quantum photonic circuits has been increasing continuously, which makes the calibration of the phase shifters on the chip increasingly difficult. For the calibration of multiple cascaded phase shifters that is not easy to be decoupled, the resources consumed by conventional brute force methods increase exponentially with the number of phase shifters, making it impossible to calibrate a relatively large number of cascaded phase shifters. In this work, we experimentally validate an efficient method for calibrating cascaded phase shifters that achieves an exponential increase in calibration efficiency compared to the conventional method, thus solving the calibration problem for multiple cascaded phase shifters. Specifically, we experimentally calibrate an integrated quantum photonic circuit with nine cascaded phase shifters and achieve a high-precision calibration with an average fidelity of 99.26%.

Keywords: cascaded phase shifters, calibration, quantum photonic chip

PACS: 42.82.–m, 03.67.–a **DOI:** 10.1088/1674-1056/ac8737

1. Introduction

By exploiting quantum mechanical effects, quantum information technologies promise significant advantages in communication,[1–5] computation,[6–11] and measurement.[12–15] Among various physical systems for quantum information processing, photons have received considerable attention because of their fast propagation speed, easy manipulation and noise immunity. Quantum information research based on optical systems have made great progress[16–31] and have achieved quantum supremacy[32–34] recently. As the complexity of optical quantum information processing tasks increases, the number of optical components required increases dramatically, which leads to a continuous increase in sizes of optical circuits, making it a natural choice to move the entire system to an integrated optical platform. So far, a variety of experiments based on integrated quantum photonic circuits have been reported, including on-chip quantum logic gates,[35] on-chip multi-photon entanglement sources,[36] and experimental demonstrations of on-chip quantum algorithms and quantum simulations.[37] The latest quantum photonic chip have integrated nearly one thousand optical components.[38]

With the increase in the size of a quantum photonic chip, it becomes increasingly difficult to calibrate the large number of phase shifters on the chip, especially for the case of multiple cascaded phase shifters that is not easy to be decoupled. For example, for the quantum photonic chip with more than 70 phase shifters presented in Ref. [39], there are multiple cascaded structures with five phase shifters that are hard to be decoupled. To calibrate these phase shifters, the authors selected 10 voltages for each phase shifter, for a total of 10^5 voltage combinations, and then fitted the sampling points accordingly. This calibration method, in which the number of sampling points increases exponentially with the number of cascaded phase shifters, is time consuming and not scalable. Similarly, for some special quantum information applications, such as blind quantum computing,[40] qubits encoded in two paths need to pass through multiple unitary transformations in succession to accomplish the specified function, and this requires cascading multiple phase shifters on the chip and calibrating these phase shifters. To solve this problem, Xing *et al.*[41] recently proposed an efficient calibration method that requires the number of sampling points to grow only linearly with the number of cascaded phase shifters.

In this work, we report an experimental demonstration of this efficient calibration method on a photonic chip. Specifically, we experimentally prepare a nine-phase shifter cascaded silicon-based quantum photonic chip and efficiently calibrate all nine phase shifters, achieving a high-precision calibration with an average fidelity of 99.26%. Our experimental results show that the number of sampling points required by using this new method increases only linearly with the number of cascaded phase shifters, achieving an exponential resource saving compared to the conventional calibration method.[39]

[†]These authors contributed equally to this work.

[‡]Corresponding author. E-mail: zhouxq8@mail.sysu.edu.cn

© 2022 Chinese Physical Society and IOP Publishing Ltd

2. Methodology

2.1. Calibration of a single phase shifter

Before describing the method of calibrating multiple cascaded phase shifters, let us first briefly review the standard method of calibrating a single phase shifter. Here we take electro-thermal phase shifters as an example, and the calibration method described in the following is also applicable to other types of phase shifters. Figure 1(a) shows a two-rail circuit consisting of an electro-thermal phase shifter and two multimode interferometers (MMIs), where MMI is used to realize the function of a beam splitter. A photon input to this circuit can encode a single qubit, with the photon encoded as $|0\rangle = \binom{1}{0}$ in the upper rail and $|1\rangle = \binom{0}{1}$ in the lower rail. The MMI should ideally have a 50:50 beam splitting ratio, but in practice there is often some deviation, so its matrix form is expressed as

$$\mathrm{MMI}(\eta) = \begin{pmatrix} \cos\eta & \mathrm{i}\sin\eta \\ \mathrm{i}\sin\eta & \cos\eta \end{pmatrix}, \tag{1}$$

where η is a constant to be determined relating to the MMI splitting ratio.

By changing the current I applied on the phase shifter, the optical path difference between the upper and lower rails can be altered, thus enabling the phase-shifting operation of the path-encoded optical qubit. The matrix form of this phase-shifting operation can be written as

$$PS(\theta) = \begin{pmatrix} 1 & 0 \\ 0 & \mathrm{e}^{\mathrm{i}\theta} \end{pmatrix}. \tag{2}$$

Here the phase θ of the phase shifter has the following relationship with the current I applied on the phase shifter[42,43]

$$\theta = \gamma I^2 + \phi, \tag{3}$$

where γ and ϕ are unknown constant parameters. The so-called calibration of the phase shifter is to confirm the specific values of γ and ϕ.

To calibrate this phase shifter, we let light input from the upper rail and measure the power output from the upper rail. The output state can be written as

$$|\psi_{\mathrm{out}}\rangle = \mathrm{MMI}(\eta)PS(\theta)\mathrm{MMI}(\eta)|0\rangle. \tag{4}$$

The ratio of the output power to the input power is the transmittance T, which can be expressed as

$$\begin{aligned} T(I) &= |\langle 0|\psi_{\mathrm{out}}\rangle|^2 = \cos^4(\eta) + \sin^4(\eta) \\ &\quad - \frac{1}{2}\sin^2(2\eta)\cos(\gamma I^2 + \phi), \end{aligned} \tag{5}$$

where η, γ and ϕ are all constants to be determined. The current I is varied experimentally and then multiple sets of T and I values are measured. As shown in Fig. 1(b), the next step is to fit the data of T and I using Eq. (5), and the values of η, γ and ϕ can be determined, thus completing the calibration of the MMI splitting ratio and the phase shifter simultaneously.

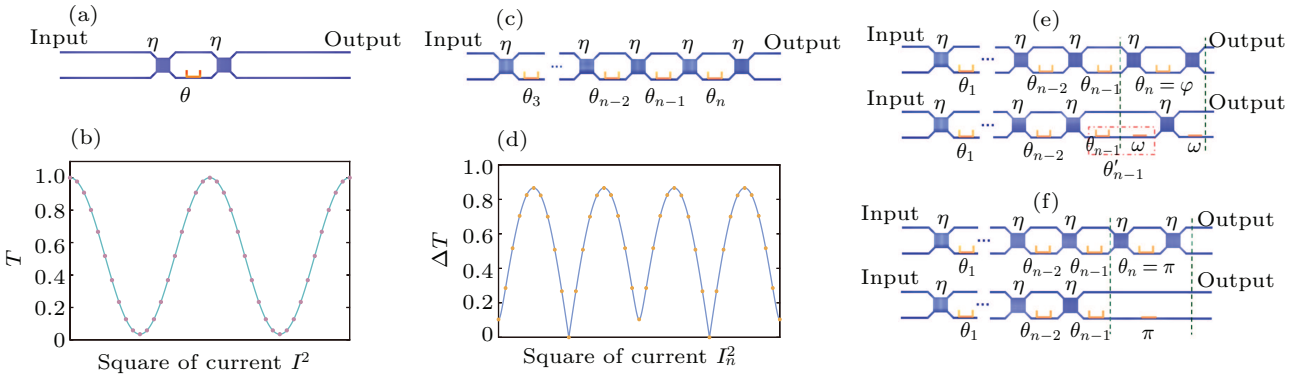


Fig. 1. Schematic diagram of the calibration method for the photonic circuit with cascaded phase shifters. (a) The photonic circuit with a single phase shifter. (b) The variation of the transmittance T with the square of the current applied on the phase shifter. (c) The photonic circuit with cascaded phase shifters. (d) The variation of the range of the transmittance ΔT with the square of the current applied on the nth phase shifter. (e) Equivalent photonic circuit for calibrating the $(n-1)$th phase shifter. (e) Equivalent photonic circuit for calibrating the $(n-2)$th phase shifter.

2.2. Calibration of cascaded phase shifters

Now let us analyze how to calibrate a circuit with multiple cascaded phase shifters. As shown in Fig. 1(c), n phase shifters are sandwiched between $n+1$ MMIs. We first describe how to calibrate the last phase shifter.

Calibration of the nth phase shifter — Inputting light from the upper rail, no matter what phases the first $n-2$ phase shifters are, the quantum state before reaching the $(n-1)$th phase shifter can always be written as $|\psi_{n-1}\rangle = \binom{\cos\alpha}{\mathrm{e}^{\mathrm{i}\delta}\sin\alpha}$. Then, $|\psi_{n-1}\rangle$ goes through the last two phase shifters and the two MMIs, and the output state obtained reads

$$|\psi_{\mathrm{out}}\rangle = \mathrm{MMI}(\eta)PS(\theta_n)\,\mathrm{MMI}(\eta)PS(\theta_{n-1})\,|\psi_{n-1}\rangle. \tag{6}$$

After calculation, the transmittance T can be expressed as

$$T(\theta_n, \theta_{n-1}) = |\langle 0|\psi_{\mathrm{out}}\rangle|^2 = A + B + C\sin\left(\theta_{n-1} + \delta'\right), \tag{7}$$

where

$$A = \frac{1}{2}\left[1 + \cos(2\alpha)\cos^2(2\eta)\right],$$

$$B = -\frac{1}{2}\cos(2\alpha)\sin^2(2\eta)\cos\theta_n,$$
$$C = \frac{\sin(2\alpha)}{2}\sqrt{1-\sin^4(2\eta)\left[\cos\theta_n - \cot^2(2\eta)\right]^2},$$
$$\delta' = \delta + \arctan\left[\frac{1}{\cos(2\eta)}\cdot\tan\left(\frac{\theta_n}{2}\right)\right]. \quad (8)$$

For a given θ_n, by traversing θ_{n-1}, one can obtain the maximum value of the transmittance $T_{\max}(\theta_n) = A + B + |C|$ and the minimum value of the transmittance $T_{\min}(\theta_n) = A + B - |C|$.

The difference between the two extreme values of transmittance is $\Delta T = 2|C|$, which is a function of θ_n. Employing $\theta_n = \gamma_n I_n^2 + \phi_n$, one can obtain

$$\Delta T(I_n) = |\sin(2\alpha)|\sqrt{1-\sin^4(2\eta)\left[\cos\left(\gamma_n I_n^2 + \phi_n\right) - \cot^2(2\eta)\right]^2}, \quad (9)$$

where α, η, γ_n, and ϕ_n are all constants to be determined. The current I_n is varied experimentally, and for each I_n, traverse I_{n-1} to measure the maximum and minimum values of the transmittance and calculate their difference ΔT.

As shown in Fig. 1(d), the data of ΔT and I_n are then fitted using Eq. (9), and the values of α, η, γ_n, and ϕ_n can be determined, thus completing the calibration of the nth phase shifter.

Calibration of other phase shifters — Let us proceed to calibrate the $(n-1)$th phase shifter. Since the nth phase shifter has been calibrated, we can set θ_n to an arbitrary phase. It can be found by calculation that when θ_n is set to φ, in which

$$\varphi = \mathrm{i}\ln\left\{\frac{1}{2}\sin^2\eta\left[-\cot^2\eta + \tan^2\eta - \mathrm{i}\sqrt{\left[1+2\cos(2\eta)\right]\csc^4\eta\sec^4\eta}\right]\right\}, \quad (10)$$

the following equation can be obtained:

$$\mathrm{MMI}(\eta)PS(\varphi)\mathrm{MMI}(\eta) = \mathrm{e}^{\mathrm{i}\varepsilon}PS(\omega)\mathrm{MMI}(\eta)PS(\omega), \quad (11)$$

where

$$\omega = -\frac{\mathrm{i}}{2}\ln\left(\frac{1-\mathrm{e}^{\mathrm{i}\varphi}\cot^2\eta}{\mathrm{e}^{\mathrm{i}\varphi}-\cot^2\eta}\right),$$
$$\varepsilon = -\mathrm{i}\ln\left(\cos\eta - \mathrm{e}^{\mathrm{i}\varphi}\sin\eta\tan\eta\right). \quad (12)$$

This means that the last two MMIs together with the nth phase shifter equivalently implement the function of a single MMI (with a fixed additional phase shift ω introduced before and after the MMI). As shown in Fig. 1(d), the $(n-1)$th phase shifter thus equivalently becomes the last phase shifter sandwiched between two MMIs and can therefore be calibrated using the method described above to identify γ_{n-1} and ϕ_{n-1}. Note that the final calibrated ϕ_{n-1} has to be subtracted from ω since a fixed additional phase shift ω is introduced.

Next we calibrate the $(n-2)$th phase shifter. Similarly, by setting $\theta_n = \pi$, we obtain

$$\mathrm{MMI}(\eta)PS(\pi)\mathrm{MMI}(\eta) = PS(\pi), \quad (13)$$

which means that the last two MMIs are equivalently removed and both the nth and $(n-1)$th phase shifters no longer have an effect on the transmittance T. As shown in Fig. 1(f), the $(n-2)$th phase shifter becomes equivalent to the last phase shifter sandwiched between two MMIs, so it can be calibrated using the method described above to identify γ_{n-2} and ϕ_{n-2}.

The remaining phase shifters can be calibrated in a similar way. For example, we set $\theta_n = \pi$ and $\theta_{n-2} = \varphi$ to calibrate the $(n-3)$th phase shifter, then we set $\theta_n = \pi$ and $\theta_{n-2} = \pi$ to calibrate the $(n-4)$th phase shifter. We can thus calibrate all the phase shifters sequentially in this reverse order. Note that the first and foremost phase shifter can be calibrated in the same way that a single phase shifter is calibrated. For a photonic chip with n cascaded phase shifters, if the number of sampling points per phase shifter is m, the total number of sampling points required using our method is $m^2 \times (n-1) + m$, which exhibits exponential improvement over the mn number of sampling points required by the traditional calibration method.

Note that the calibration method described above is a modified version of the scheme in Ref. [41]. The original scheme in Ref. [41] mainly considers the scenario where the splitting ratio of the MMI is exactly 50 : 50, in which case the calibrated phase would have an undetermined phase difference of 0 or π, and further operations are needed to determine this phase difference. In contrast, our modified scheme assumes that the splitting ratio of the MMI is not strictly 50 : 50, which is usually consistent with the practical situation.[41] In this case, our modified method can directly distinguish between the two phase differences of 0 and π, thus further simplifying the calibration procedure.

3. Experiment

To experimentally validate this calibration method for cascaded phase shifters, we prepared a silicon photonic chip with nine phase shifters cascaded as shown in Fig. 2(a) (see Appendix A).

We send a laser beam into the chip from the upper left port and measure the optical power output from the upper right port to calculate the transmittance T. Next, the current I_8 of the 8th phase shifter and the current I_9 of the 9th phase shifter are jointly traversed to investigate the variation of the transmittance T, where I_8 has been chosen with 38 different values and I_9 has been chosen with 50 different values. As shown in Fig. 2(b), 50 sets of ΔT and I_9 are obtained and then fitted with Eq. (2), which results in $\gamma_9 = 0.2204$, $\phi_9 = 5.8187$ and $\eta = 0.7630$, completing the 9th phase shifter calibration. The

η value here is 0.7630, which corresponds to the splitting ratio of MMI as 52.24:47.76. After the experimental testing, it is found that the difference of the splitting ratio between different MMIs on the chip is within one percent, so the η value is set to 0.7630 during the whole calibration process. Based on the value of η, we obtain $\varphi = 1.614$ by using Eq. (10). As shown in Fig. 2(c), we then set $\theta_9 = 1.614$ and jointly traverse the currents I_7 and I_8 to derive $\gamma_8 = 0.2229$ and $\phi_8 = 5.5536$. Next, we set $\theta_9 = \pi$ and jointly traverse the currents I_6 and I_7 to derive $\gamma_7 = 0.2198$ and $\phi_7 = 5.3965$, which is shown in Fig. 2(d). In a similar way, we complete the calibration of the 6th, 5th, 4th, 3rd and 2nd phase shifters in turn as shown in Figs. 2(e)–2(i), and obtain

$$\begin{aligned} \gamma_6 &= 0.2248, \quad \phi_6 = 5.8808, \\ \gamma_5 &= 0.2219, \quad \phi_5 = 5.0105, \\ \gamma_4 &= 0.2234, \quad \phi_4 = 6.1118, \\ \gamma_3 &= 0.2248, \quad \phi_3 = 7.2625, \\ \gamma_2 &= 0.2187, \quad \phi_2 = 5.0941. \end{aligned} \tag{14}$$

Finally we set $\theta_9 = \pi$, $\theta_7 = \pi$, $\theta_5 = \pi$ and $\theta_3 = \pi$ and then scan I_1 alone, where I_1 has been chosen with 40 different values. As shown in Fig. 2(j), by using the method of calibrating a single phase shifter, we get $\gamma_1 = 0.2237$ and $\phi_1 = 3.9150$, thus completing the calibration of all phase shifters. In our experiment, only $8 \times 38 \times 50 + 40 = 15240$ data points were collected in total to complete the calibration. If the traditional calibration method[39] is adopted, even if only 6 different values are selected for each phase shifter, 10077696 data points need to be collected to complete the calibration, which is three orders of magnitude higher than the data points needed by using our method.

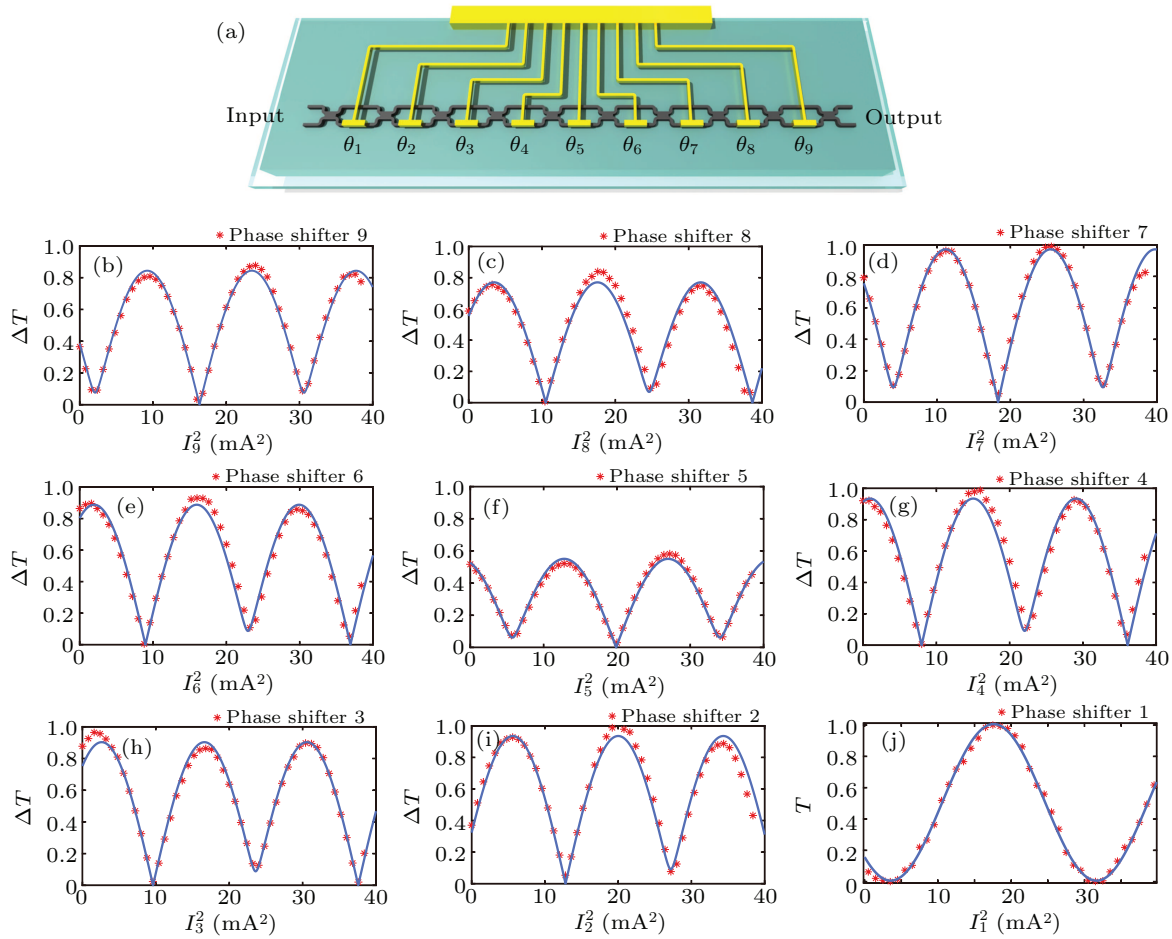


Fig. 2. Schematic of the experimental setup and the measured results for the calibration of the phase shifters. (a) A silicon quantum photonic chip cascaded with nine phase shifters. (b)–(j) The calibration experimental data of the nine phase shifters in reverse order. The calibration of the second to the ninth phase shifters is carried out by fitting the range of the transmittance ΔT with the square of the current applied on the corresponding phase shifter. The calibration of the first phase shifter is conducted by fitting the transmittance T with the square of the current applied on the first phase shifter.

After completing the calibration of the phase shifter, the following tests are performed on the chip to verify the accuracy of the calibration. We apply a random current between 2 mA and 5.5 mA to each phase shifter, and measure the experimentally observed transmittance T_{exp}. This is then compared with the transmittance T_{pre} we predict from the calibration results. The fidelity of the two transmittances is defined as[44]

$$F = \sqrt{T_{\text{exp}} T_{\text{pre}}} + \sqrt{(1 - T_{\text{exp}})(1 - T_{\text{pre}})}. \tag{15}$$

We repeated the above test 1000 times and calculated 1000 fidelity values. As shown in Fig. 3, 938 out of 1000 fidelity values are more than 98%, and the average value of all fidelities is 99.26%, which shows that our calibration results of the phase shifters are in good agreement with the experimental observations. The non-perfect calibration results are mainly caused by signal jitter of the electronic controller and thermal crosstalk on the photonic chip. The deviation of the calibration value of the previous phase shifter from the actual value will also bring some errors to the subsequent calibration.

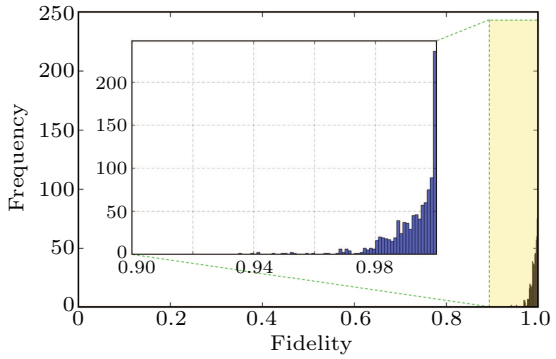


Fig. 3. Statistical fidelity of the transmittance of the chip. The histogram shows the distribution of statistical fidelity between the predicted and the measured transmittance, over 1000 sets of nine randomly selected currents. Here, 93.8% of the measured transmittance has a fidelity higher than 98%.

Our method can be straightforwardly extended to the case in which the splitting ratios of the MMIs are different (see Appendix B). However, since the differences in the splitting ratios of the MMIs on this chip are small,[45] fitting the data with the formula that distinguishes between the splitting ratios yields the results with a lower fidelity than the formula that does not distinguish between the splitting ratios. Therefore, in this experiment, we still use a fitting formula that ignores the difference in the splitting ratios of different MMIs.

4. Conclusion

In this work, we have experimentally validated an efficient method for calibrating large-scale cascaded phase shifters.

Specifically, we experimentally calibrated an integrated quantum photonic chip with nine cascaded phase shifters and achieved a high-precision calibration with an average fidelity of 99.26%. Our experimental results show that the number of sampling points required by using this new method increases only linearly with the number of cascaded phase shifters, achieving an exponential speedup compared to the conventional calibration method. This technique has the potential to be widely used in the field of integrated photonic quantum information processing.

Appendix A: Fabrication of the chip

The chip was fabricated on a 220 nm silicon-on-insulator (SOI) wafer. Electron beam direct writing and inductively coupled plasma etching were used to construct grating couplers and waveguides. The fabricated chip was then insulated with a 1.2 μm layer of SiO_2. Then, above the particular area, 150-nm nichrome was patterned to operate as heaters. Lastly, 10-nm Ti and 200-nm Au were patterned as the electrodes.

Appendix B: The case of different splitting ratios of MMIs

As shown in Fig. B1, the splitting ratio parameters of the two MMIs before and after the nth phase shifter are η_{n-1} and η_n, respectively. The quantum state before reaching the $(n-1)$th phase shifter can always be written as $\binom{|\psi_{n-1}\rangle=\cos\alpha}{e^{i\delta}\sin\alpha}$. Then, $|\psi_{n-1}\rangle$ goes through the last two phase shifters and the two MMIs, and the output state obtained is

$$|\psi_{\text{out}}\rangle = BS(\eta_{n-1})PS(\theta_n)BS(\eta_n)PS(\theta_{n-1})|\psi_{n-1}\rangle. \quad \text{(B1)}$$

After the calculation, the transmittance T can be expressed as

$$\begin{aligned} T(\theta_n,\theta_{n-1}) &= |\langle 0|\psi_{\text{out}}\rangle|^2 \\ &= A'+B'+C'\sin\left(\theta_{n-1}+\delta''\right), \end{aligned} \quad \text{(B2)}$$

where

$$\begin{aligned} A' &= \frac{1}{2}\left[1+\cos(2\alpha)\cos(2\eta_{n-1})\cos(2\eta_n)\right], \\ B' &= -\frac{1}{2}\cos(2\alpha)\sin(2\eta_{n-1})\sin(2\eta_n)\cos(\theta_n), \\ C' &= \frac{\sin(2\alpha)}{2}\cdot\sqrt{1-\sin^2(2\eta_{n-1})\sin^2(2\eta_n)\left[\cos\theta_n-\cot(2\eta_{n-1})\cot(2\eta_n)\right]^2}, \\ \delta'' &= \delta+\arctan\left[\frac{\sin(\theta_n)}{\cos(2\eta_{n-1})\cos\theta_n+\cot(2\eta_n)\sin(2\eta_{n-1})}\right]. \end{aligned} \quad \text{(B3)}$$

For a given θ_n, by traversing θ_{n-1}, one can obtain the maximum value of the transmittance $T_{\max}(\theta_n)=A'+B'+|C'|$ and the minimum value of the transmittance $T_{\min}(\theta_n)=A'+B'-|C'|$.

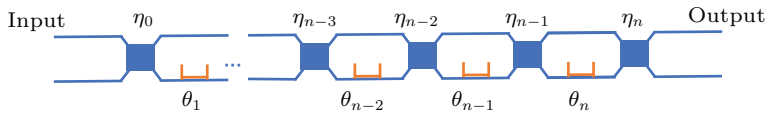


Fig. B1. The photonic circuit with cascaded phase shifters. Different MMIs have different splitting ratio parameters η_0, η_1, …, η_{n-1} and η_n.

The difference between the two extreme values of transmittance is $\Delta T = 2|C'|$, which is a function of θ_n. Substituting $\theta_n = \gamma_n I_n^2 + \phi_n$, one can obtain

$$\Delta T(I_n) = |\sin(2\alpha)|\sqrt{1-\sin^2(2\eta_{n-1})\sin^2(2\eta_n)\cdot[\cos(\gamma_n I_n^2+\phi_n)-\cot(2\eta_{n-1})\cot(2\eta_n)]^2}, \tag{B4}$$

where α, η_n, η_{n-1}, γ_n, and ϕ_n are all constants to be determined. The current I_n is varied experimentally, and for each I_n, traverse I_{n-1} to measure the maximum and minimum values of the transmittance and calculate their difference ΔT. The data of ΔT and I_n are then fitted using Eq. (B4), and the values of α, η_n, η_{n-1}, γ_n and ϕ_n can be determined, thus completing the calibration of the nth phase shifter. The remaining phase shifters can be calibrated sequentially in the reverse order in a similar way.

Acknowledgements

Project supported by the National Key Research and Development Program of China (Grant No. 2017YFA0305200), the Key Research and Development Program of Guangdong Province, China (Grant Nos. 2018B030329001 and 2018B030325001), and the National Natural Science Foundation of China (Grant No. 61974168).

References

[1] Gisin N, Ribordy G, Tittel W and Zbinden H 2002 *Rev. Mod. Phys.* **74** 145
[2] Xu F H, Ma X F, Zhang Q, Lo H K and Pan J W 2020 *Rev. Mod. Phys.* **92** 025002
[3] Wei K J, Li W, Tan H, Li Y, Min H, Zhang W J, Li H, You L X, Wang Z, Jiang X, Chen T Y, Liao S K, Peng C Z, Xu F H and Pan J W 2020 *Phys. Rev. X* **10** 031030
[4] Yin J, Li Y H and Liao S K 2020 *Nature* **582** 501
[5] Bennett C H and Brassard G 1984 *Proceedings of IEEE International Conference on Computers, Systems, and Signal Processing*, December 9–12, 1984, Bangalore, India, p. 175
[6] Ladd T D, Jelezko F, Laflamme R, Nakamura Y, Monroe C and O'Brien J L 2010 *Nature* **464** 45
[7] Zhong H S, Wang H, Deng Y H, *et al.* 2020 *Science* **370** 1460
[8] Bentivegna M, Spagnolo N, Vitelli C, Flamini F, Viggianiello N, Latmiral L, Mataloni P, Brod J D, Galvao F E, Crespi A, Ramponi R, Osellame R and Sciarrino F 2015 *Sci. Adv.* **1** e1400255
[9] Ciampini M A, Orieux A, Paesani S, Sciarrino F, Corrielli G, Crespi A, Ramponi R, Osellame R and Mataloni P 2016 *Light: Sci. Appl.* **5** e16064
[10] Shor P W 1994 *Proceedings 35th Annual Symposium on Foundations of Computer Science*, November 20–22, 1994, Santa Fe, NM, USA, p. 124
[11] Grover L K 1997 *Phys. Rev. Lett.* **79** 325
[12] Ahluwalia D V 1994 *Phys. Lett. B* **339** 4
[13] Huttner B, Muller A, Gautier J D, Zbinden H and Gisin N 1996 *Phys. Rev. A* **54** 3783
[14] Raussendorf R, Browne D E and Briegel H J 2003 *Phys. Rev. A* **68** 022312
[15] Kim Y S, Lee J C, Kwon O and Kim Y H 2012 *Nat. Phys.* **8** 117
[16] Chen Z X, Li J L, Song Q C, Wang H, Zangi S M and Qiao C F 2017 *Phys. Rev. A* **96** 062123
[17] Chen Z X, Wang H, Li J L, Song Q C and Qiao C F 2019 *Sci. Rep.* **9** 5687
[18] Pan J W, Chen Z B, Lu C Y, Weinfurter H, Zeilinger A and Zukowski M 2012 *Rev. Mod. Phys.* **84** 777
[19] Kwiat P G, Mattle K, Weinfurter H, Zeilinger A, VSergienko A and Shih Y 1995 *Phys. Rev. Lett.* **75** 4337
[20] Bouwmeester D, Pan J W, Daniell M, Weinfurter H and Zeilinger A 1999 *Phys. Rev. Lett.* **82** 1345
[21] Pan J W, Daniell M, Gasparoni S, Weihs G and Zeilinger A 2001 *Phys. Rev. Lett.* **86** 4435
[22] Zhao Z, Chen Y A, Zhang A N, Yang T, Briegel H J and Pan J W 2004 *Nature* **430** 54
[23] Walther P, Resch K J, Rudolph T, Schenck E, Weinfurter H, Vedral V, Aspelmeyer M and Zeilinger A 2005 *Nature* **434** 169
[24] Lu C Y, Zhou X Q, Guhne O, Gao W B, Zhang J, Yuan Z S, Goebel A, Yang T and Pan J W 2007 *Nat. Phys.* **3** 91
[25] Wieczorek W, Krischek R, Kiesel N, Michelberger P, Toth G and Weinfurter H 2009 *Phys. Rev. Lett.* **103** 020504
[26] Prevedel R, Cronenberg G, Tame M S, Paternostro M, Walther P, Kim M S and Zeilinger A 2009 *Phys. Rev. Lett.* **103** 020503
[27] Yao X C, Wang T X, Xu P, Lu H, Pan G C, Bao X H, Peng C Z, Lu C Y, Chen Y A and Pan J W 2012 *Nat. Photon.* **6** 225
[28] Wang X L, Chen L K, Li W, Huang H L, Liu C, Chen C, Luo Y H, Su Z E, Wu D, Li Z D, Lu H, Hu Y, Jiang X, Peng C Z, Li L, Liu N L, Chen Y A, Lu C Y and Pan J W 2016 *Phys. Rev. Lett.* **117** 210502
[29] Chen L K, Li Z D, Yao X C, Huang M, Li W, Lu H, Yuan X, Zhang Y B, Jiang X, Peng C Z, Li L, Liu N L, Ma X F, Lu C Y, Chen Y A and Pan J W 2017 *Optica* **4** 77
[30] Zhong H S, Li Y, Li W, Peng L C, Su Z E, Hu Y, He Y M, Ding X, Zhang W J, Li H, Zhang L, Wang Z, You L X, Wang X L, Jiang X, Li L, Chen Y A, Liu N L, Lu C Y and Pan J W 2018 *Phys. Rev. Lett.* **121** 250505
[31] Wang X L, Luo Y H, Huang H L, Chen M C, Su Z E, Liu C, Chen C, Li W, Fang Y Q, Jiang X, Zhang J, Li L, Liu N L, Lu C Y and Pan J W 2018 *Phys. Rev. Lett.* **120** 260502
[32] Boixo S, Isakov S V, Smelyanskiy V N, Babbush R, Ding N, Jiang Z, Bremner M J, Martinis J M and Neven H 2018 *Nat. Phys.* **14** 595
[33] Guo C, Liu Y, Xiong M, Xue S, Fu X, Huang A, Qiang X, Xu P, Liu J, Zheng S, Huang H, Deng M, Poletti D, Bao W S and Wu J J 2019 *Phys. Rev. Lett.* **123** 190501
[34] Hangleiter D, Kliesch M, Eisert J and Gogolin C 2019 *Phys. Rev. Lett.* **123** 190501)
[35] Politi A, Cryan M J, Rarity J G, Yu S and O'Brien J L 2008 *Science* **320** 646
[36] Wang J, Paesani S, Santagati R, Knauer S, Gentile A A, Wiebe N, Petruzzella M, O'Brien J L, Rarity J G, Laing A and Thompson M G 2017 *Nat. Phys.* **13** 551
[37] Spring J B, Metcalf B J, Humphreys P C, Kolthammer W S, Jin X M, Barbieri M, Datta A, Nicholas T P, Langford N K, Kundys D, Gates J C, Smith B J, Smith P G R and Walmsley I A 2013 *Science* **339** 798)

[38] Wang J W, Sciarrino F, Laing A and Thompson M G 2020 *Nat. Photon.* **14** 273
[39] Qiang X G, Zhou X Q, Wang J W, Wilkes C M, Loke T, O'Gara S, Kling L, Marshall G D, Santagati R, Ralph T C, Wang J B, O'Brien J L, Thompson M G and Matthews J C F 2018 *Nat. Photon.* **12** 534
[40] Childs A M 2005 *Quantum Physics* **5** 456
[41] Xing Z Y, Li Z H, Feng T F and Zhou X Q 2021 *Acta Phys. Sin.* **70** 184207 (in Chinese)
[42] Kang G, Kim S H, You J B, Lee D S, Yoon H, Ha Y G, Kim J H, Yoo D E, Lee D W, Youn C H, Yu K and Park H H 2019 *IEEE Photon. Technol. Lett.* **31** 1685
[43] Sun J, Timurdogan E, Yaacobi A, *et al.* 2013 *Nature* **493** 195
[44] Qiang X G, Loke T, Montanaro A, Aungskunsiri K, Zhou X Q, O'Brien J L, Wang J B and Matthews J C F 2016 *Nat. Commun.* **7** 11511
[45] The splitting ratios of 10 MMIs on a test chip are measured and they all range from 52.19:47.81 to 52.98:47.02